Int J Appl Earth Obs Geoinformation 91 (2020) 102152

Contents lists available at ScienceDirect

Int J Appl Earth Obs Geoinformation

journal homepage: www.elsevier.com/locate/jag

A novel approach to optimize hierarchical vegetation mapping from hyper-temporal NDVI imagery, demonstrated at national level for Namibia

Eduard Westinga[a,*], Ana Patricia Ruiz Beltran[a], Cees A.J.M. de Bie[a], Hein A.M.J. van Gils[b,c]

[a] Department of Natural Resources, Faculty ITC, University of Twente, Enschede, the Netherlands
[b] Department of Geography, Geoinformatics and Meteorology, Faculty of Natural and Agricultural Sciences, University of Pretoria, Hatfield, South Africa
[c] College of Wildlife Resources, Northeast Forestry University (NEFU), Harbin, PR China

ARTICLE INFO

Keywords:
Temporal NDVI-profile
Dendrogram
Hierarchy
Vegetation map
Biome
Ecoregion
SPOT-VGT-MVC
ISODATA clustering

ABSTRACT

This paper presents a novel methodological approach to countrywide vegetation mapping. We used green vegetation biomass over the year as captured by coarse resolution hyper-temporal NDVI satellite-imagery, to generate vegetation mapping units at the biome, ecoregion and at the next lower hierarchical level for Namibia, excluding the Zambezi Region. Our method was based on a time series of 15 years of SPOT-VGT-MVC images each representing a specific 10-day period (dekad). The ISODATA unsupervised clustering technique was used to separately create 2–100 NDVI-cluster maps. The optimal number of temporal NDVI-clusters to represent the information on vegetation contained in the imagery was established by divergence separability statistics of all generated NDVI-clusters. The selected map consisted of legend of 81 cluster-specific temporal NDVI-profiles covering each a 15-year period of averaged NDVI data representing all pixels classified to that cluster. Then, by legend-entry using the dekad-medians of all 15 annual repeats, we produced generalized legend-entries without year-specific anomalies for each cluster. Subsequently, a hierarchical cluster analysis of these temporal NDVI-profiles was used to produce a dendrogram that generated grouping options for the 81 legend-entries. Maps with cluster-groups of 8 and 4 legend-entries resulted. The 81-cluster map and its 65 legend-entries vector version have no equivalent in published vegetation maps. The 8 cluster-group map broadly corresponds with published ecoregion level maps and the 4 cluster-group map with the published biome maps in their number of legend units. The published vegetation maps varied considerably from our NDVI-profile maps in the location of mapping unit boundaries. The agreement index between our map and published biome maps ranges from 70 − 93. For the ecoregion level, the agreement index is much lower, namely 51 − 75. Our methodological approach showed a considerably higher discretionary power for hierarchical levels and the number of vegetation mapping units than the approaches applied to previously published maps. We recommended an approach to transform our three hyper-temporal NDVI-profiles based legend-entries into more specific vegetation units. This might be accomplished by re-analysis of available, spatially-comprehensive plant species occurrence data.

1. Introduction

Vegetation unit maps covering Namibia have been published every decade since the 1970s (Table 1). The maps appear to be based on informal classifications of unreported ground observation, followed by the spatial extrapolation of the distinguished classes and class complexes using expert knowledge. Since the turn of this century, hyper-temporal NDVI satellite imagery have been used in combination with other data and expert knowledge in the production of a published map of Namibia (Table 1: last row) and for a portions of the country (Wagenseil and Samimi, 2007; Hüttich et al., 2009). Unfortunately, these mapping procedures are hard to replicate consistently and are prohibitively time-consuming for countrywide maps (van Gils et al., 2008). Across existing Namibian vegetation maps, the unit boundaries in the map image, the number of mapping units, and the hierarchy of the legend units differ substantially. In addition, the nomenclature of the two hierarchical levels represented in the Namibian map set shows a wide variety (Table 1). For nomenclature, we adopt biome (2–6 units) and ecoregion levels (≥ 8 − 20 units) for Namibia in this paper. In neighbouring South Africa and globally, vegetation units have been mapped at the biome level (Wessels et al., 2011; Higgins et al., 2016) or ecoregion level (Mayaux et al., 2004). All three studies covered a much larger area than Namibia and selected the biome or ecoregion as the exclusive hierarchical mapping unit level. Among the published

* Corresponding author.
E-mail address: e.westinga@utwente.nl (E. Westinga).

https://doi.org/10.1016/j.jag.2020.102152
Received 27 August 2019; Received in revised form 27 March 2020; Accepted 30 April 2020
Available online 13 May 2020

Table 1
Published vegetation maps of Namibia and their number of legend units at the biome and ecoregion level. The labels of the legend units were taken from the published maps.

Author	Year	Label in source	No. of units		Label in source	Source
		Biome level	Biome	Ecoregion	Ecoregion level	
Giess	1971	vegetation zone	3	14	vegetation type	download
Leser	1976	Florenregion	2	14	vegetation formation	digitized
White	1983	phytochoria	3	10	vegetation type	digitized
Cowling et al.	1997	biome	4	.	.	digitized
Mendelsohn et al.	2002a/b	biome	6/5*	(26)	vegetation type	download
Mendelsohn et al.	2002c	.	.	11	vegetation structure	download
Mayaux et al.	2004	.	.	10	vegetation structure	download
WWF	2011	biome	3/2*	10	ecoregions	download

* With/Without an Etosha salt pan biome; (26) number of units beyond ecoregion level.

vegetation maps of Namibia, none includes a nested, spatial hierarchy of vegetation mapping units and none provides countrywide spatial detail on vegetation contained in the available hyper-temporal satellite imagery. Moreover, none of published maps was accompanied by a reproducible mapmaking method. In our research, we extracted the number of mapping units and their hierarchical level from hyper-temporal NDVI imagery in an attempt to produce more detailed and reproducible vegetation maps.

We stacked 15-year, 10-day (dekad) SPOT NDVI data resulting in 564 values per pixel. After standard image preprocessing, we separately created 2–100 NDVI-cluster maps using unsupervised ISODATA (Tou and Gonzalez, 1974). The map with the optimal number of clusters was identified with divergence separability statistics (Swain, 1973; Girma et al., 2016). For the identified map, the median of all annual repeats by dekad (i.e. 15–16 entries per annum) was computed; these represent cluster-specific annual, temporal, dekad-medians NDVI-profiles, hereafter NDVI-profiles (Mayaux et al., 2004; Nguyen et al., 2011; Mugabowindekwe et al., 2018). The profiles were graphically visualized. Next, Hierarchical Clustering Analysis (Ali et al., 2013) was applied to the set of temporal NDVI-profiles to create a dendrogram of the hierarchical levels between clusters and defining cluster-groups. Subsequently, we compared the resulting NDVI-clusters and cluster-groups with the published vegetation maps and the annual rainfall zone maps. The comparison was made visually for the boundaries within the map image. For calculation of the agreement between the positions of mapping units we applied the confusion matrix method (Lillesand et al., 2004).

2. Method

2.1. Namibia

Namibia is situated along the Atlantic seaboard of southwest Africa (Fig. 1), centered approximately on the Tropic of Capricorn. It covers an area of approximately 825 000 km^2, and is roughly rectangular in shape, with a narrow extension along the Zambezi river in the northeast. For practical purposes, this research delineated a rectangle (hereafter Namibia) that contains almost the entire extent of the country. Only the Zambezi Region, historically known as the Caprivi-strip, was excluded. Namibia is bisected in to two zonobiomes, namely a subtropical, arid zone in the south and along the entire coast, and a tropical sub-humid, summer-rain zone in the north and northeast (Walter, 1976). More detailed biome maps (Table 1) show three to four spatial units, namely the coastal Namib Desert (Fig. 1: black 0 − 500 m) to the west of the continental escarpment (Fig. 1: dark grey 501 − 1000 m), the Nama-Karoo semi-desert on the plateau (Fig. 1: grey 1001 − 1500 m) in the south, the savanna of the Mega-Kalahari on the plateau in the northeast and the relatively small edaphic desert (Etosha salt pan) in the central-north. These biome maps differ in their unit boundaries and subdivisions as well as in the identification of smaller additional biomes at the fringes of the country. These include the coastal Succulent Karoo in the southwest, the seasonally flooded, cultivated Cuvelai basin in the central-north, and forest or woodland in the northeast. The Namib Desert and Etosha salt pan are state land and zoned as protected areas. The Nama-Karoo and the central Mega-Kalahari are parceled out into large, fenced freehold farms (van Gils et al., 2015). The northern portion of Mega-Kalahari is zoned as communal land and contains mostly unfenced agro-pastoral small-holdings. Most of the freehold farms are covered by semi-natural savanna vegetation and are used as livestock and/or wildlife ranches (e.g. van Gils et al., 2015). Crop cultivation on freeholds is only widespread in the maize-triangle between Grootfontein, Tsumeb (Fig. 1: T) and Otavi. Consequently, the vegetation cover east of the continental escarpment has been shaped in the past century by sheep and/or cattle farming, in particular by opening up grazing land by boreholes (van Gils et al., 2015) and subsequent selective grazing, purposive burning and wildfire control, bush encroachment and de-bushing. For additional info and a comprehensive overview of the current knowledge on climate and vegetation, the reader is referred to the Atlas of Namibia (Mendelsohn et al., 2002).

At its northern and southern borders, Namibia is endowed with permanent, but unnavigable rivers. The Kunene, Kwando and Kavango in the north are shared with Angola; the Orange River in the south with South Africa. The Kunene and Orange rivers are used for hydropower generation and show untapped potential for further hydropower and irrigation development.

Namibia has about 3 million inhabitants, implying a very low overall density of about 3 persons per square km. However, the majority of the population is concentrated in three areas, namely the northern agro-pastoral communal land zone (van Gils et al., 2015), the coastal Walvis Bay/Swakopmund harbor-mining-industrial-tourist hub (Fig. 1: WB) and the central Windhoek-Okahandja conurbation (Fig. 1: W). The inequality (Gini index about 60) and unemployment ($\geq$20 %) rates are extremely high.

The economic foundation of Namibia is mining; especially off-shore and onshore diamond mining, but uranium, copper, zinc and gold mining also contribute. There is additional potential in the exploitation of phosphate and hydrocarbon reserves in the marine Exclusive Economic Zone of Namibia. The second biggest contributor to the Namibian economy is the export-oriented, deep sea fishing industry. Nature-based tourism is the third economic pillar.

2.2. Materials and methods

As source of NDVI-imagery, we used the 1 km resolution SPOT-VGT-MVC data covering the 36 dekads from 1st May 1998 to 31st December 2013 [https://land.copernicus.vgt.vito.be/PDF/portal/Application.html#Home]. The SPOT-data were provided in Digital Number format (DN; one byte). The NDVI was calculated from the DN value as follows: NDVI = 0.004 DN − 0.1 (FAO, 2017). The imagery was

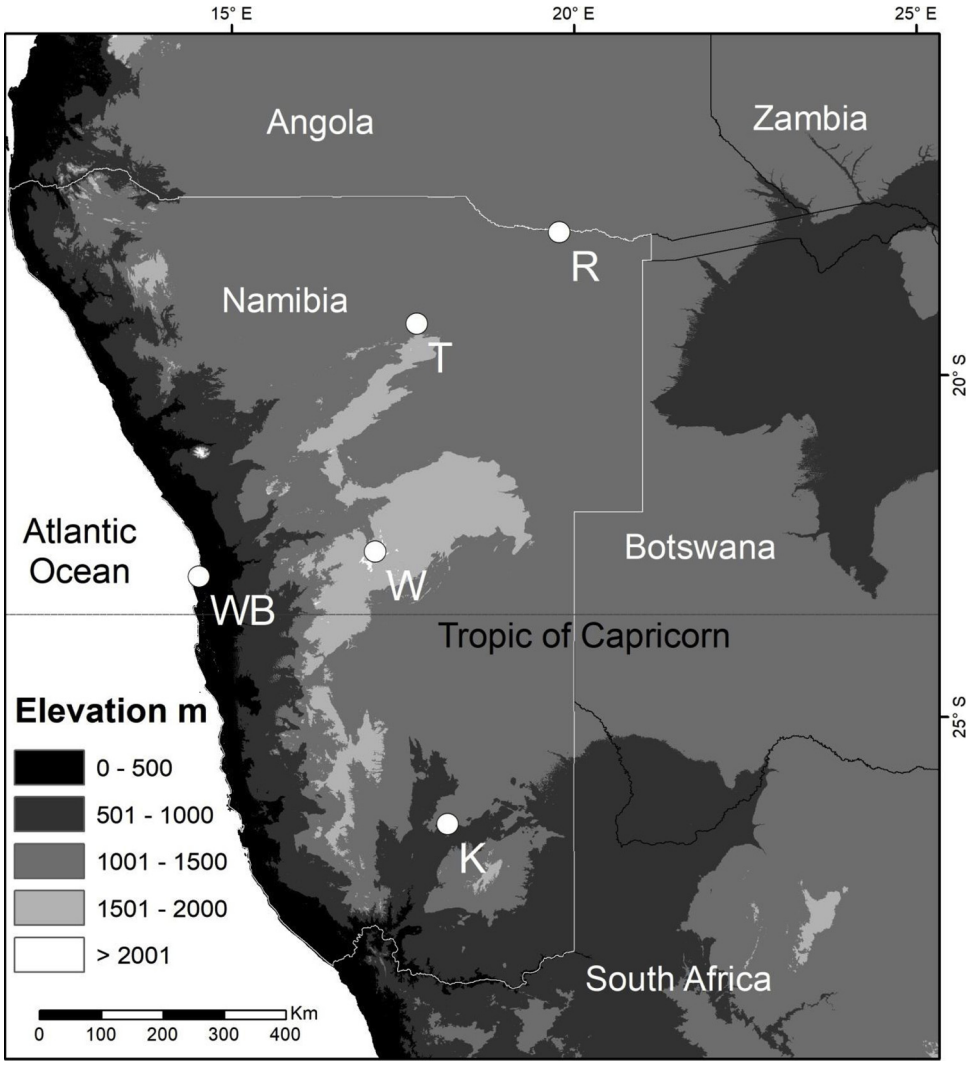

Fig. 1. Location map of Namibia. Abbreviations of towns: K = Keetmanshoop, R = Rundu, T = Tsumeb, W = Windhoek and WB = Walvis Bay. Topography source: Mendelsohn et al. (2002); DEM source: http://srtm.csi.cgiar.org/srtmdata.

projected in Plate Carree and the WGS84 spheroid and datum. We stacked all 564 images into a xyt-datacube and removed clouds and data artefacts through an upper envelop filter (Adaptive Savitzky-Golay). The filter replaced all downward peaks and missing values with estimates obtained through polynomial regression of several earlier and later NDVI-values of pixel-specific data series.

We clustered the 564 pixel values using ISODATA as embedded in ERDAS Imagine. The clustering was repeated 99 times to create a range from 2–100 NDVI-clusters (de Bie et al., 2011). Next, the statistically optimal number of clusters was selected through the use of divergence separability statistics (Swain, 1973; Girma et al., 2016). For each cluster, the average separability between clusters was calculated and plotted. The number of clusters with the highest positive deviation from the trend line connecting clusters was considered optimal (Ali et al., 2013; de Bie et al., 2012; Khan et al., 2010). To reduce the effect of extremely dry or wet years on NDVI-values, the median of all annual repeats by dekad (i.e. 15–16 entries per annum) was calculated for the identified optimal number of clusters. Subsequently, cluster-specific NDVI-profiles were generated (Nguyen et al., 2011) and graphically visualized. Hierarchical Clustering Analysis (Ali et al., 2013) was carried then out for the set of temporal NDVI-profiles of the map with the optimal number of clusters to obtain a dendrogram of clusters-groups at one or more hierarchical levels.

The cluster-group maps, i.e. the biome and ecoregion levels, were overlaid in ArcGIS and compared with published vegetation maps at the same hierarchical level (Table 1). For this purpose, the analogue vector maps were digitized. Our NDVI-profile based maps and the Mayaux et al. (2004) map were vectorized and clipped with the boundary of Namibia. For map comparison purposes, the 1: 7 million scale of the vegetation map in the Atlas of Namibia (Mendelsohn et al., 2002) was adopted. At this scale, the smallest mapable unit is 5×5 mm. (Westinga, 1989, 2004; van Gils et al., 2014). Therefore, units consisting of patches smaller than 1225 km^2 were eliminated before the comparison. The position of the biome and ecoregion boundaries was visually compared. For a quantitative comparison of maps, we intersected each of the published maps (Table 1) with our equivalent biome and ecoregion maps. We calculated the common area extent of legend units in the intersect and summarized the results in a confusion matrix (Lillesand et al., 2004). In order to calculate the overall agreement legend units of both maps has be paired by combining legend units. In addition, we also compared the climatic zone map (Namibia Resource Consultants, 1999) with our ecoregion map following the same procedures.

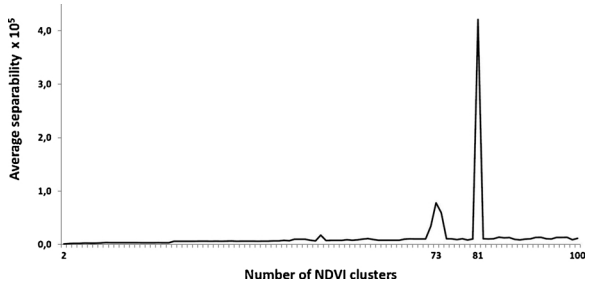

Fig. 2. The line represents the average separability of the 99 ISODATA-generated NDVI-clusters. Peak separability is reached at 81 clusters.

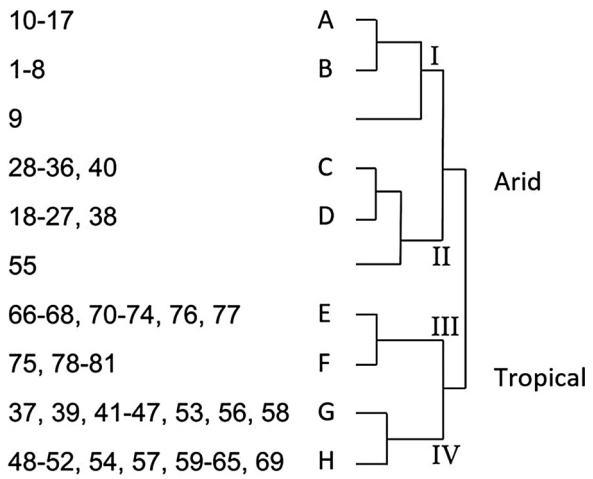

Fig. 3. The dendrogram depicts from right to left, the nested hierarchy of Arid versus Tropical, 4 (I-IV) and 8 (A-H) NDVI-profile cluster-groups of the 81 optimal NDVI-clusters. Arid versus Tropical represents the zonobiomes of Walter (1976), the I-IV level corresponds with biomes and the A-H level with ecoregions of the published vegetation maps (Table 1). Two ungrouped clusters (9 and 55) were eliminated.

3. Results

3.1. Temporal NDVI-clusters and cluster-groups dendrogram

The separability graph shows a peak at 81 NDVI-clusters (Fig. 2). None of the published vegetation maps (Table 1) shows such a high number of mapping units. The dendrogram (Fig. 3) shows three hierarchical levels of 81 (the singular, small clusters 9 and 55 were eliminated), 8 (A-H) and 4 (I-IV) mapping units respectively. The second level of 8 cluster-groups represents the ecoregions and the 4 cluster-groups represent the biomes of the published maps (Table 1).

3.2. Biome level

The overlay of the NDVI-profile based biome map (I-IV) and the published biome level vegetation maps is presented in Fig. 4. The published biome level maps include 2–5 mapping units excluding the Etosha saltpan as a separate biome (Table 1). The map with 2 biomes separates the arid from the tropical (Fig. 4: black boundary), as all published biome maps of Namibia (Table 1) do to some degree. The two large biomes correspond to the zonobiomes of Walter (1976), briefly described in the Introduction. Three other published maps present a similar boundary between the arid and the tropical biomes (Fig. 4: red, green and purple boundaries). However, Giess draws an elevational boundary between the two in the south closer to the Atlantic, roughly along the continental escarpment, i.e. separating the thermally oceanic climate from the continental climate of the plateau (Fig. 4: blue boundary). The outlier for the main biome boundaries is presented on the WWF map (Fig. 4: orange boundary). The WWF division of desert-and-shrubland versus savanna follows more or less the isohyet of 400 mm annual rainfall (Namibia Resource Consultants, 1999). Additional biomes (Table 1) are obtained by subdivision of the large tropical biome (blue, purple and red) and/or splitting the large arid biome (green) into two (Fig. 4). The highest number of biomes (5) results from a further distinction of a separate Succulent Karoo biome at the southern edge of the Namib Desert (Fig. 4: purple) in addition to splitting both large biomes.

The biome boundaries in the published maps differ substantially in their position (Fig. 4). However, a bundle of biome boundary lines (blue, green and purple) is found along the continental escarpment, more so (plus black and red) north of the Tropic of Capricorn. The bundle of vector map boundaries match more or less with I/II (black/grey) and II/IV (grey-white) boundaries of the NDVI-profile map. In contrast, three boundary lines in the northeastern portion of the country are drawn widely apart (Fig. 4: red, orange and blue). In this area, the WWF (orange) seems to have compiled their savanna biome boundary from earlier maps (Fig. 4: red and blue). Further, we note that the NDVI-profile based biome boundary between IV and III differs substantially from the biome boundaries in the published maps (Fig. 4). Similarly, the II/IV boundary from east to west in the center of map deviates from the bundle of boundaries that follow a northwest to southeast direction (Fig. 4: black, green, purple and red).

The positional agreement between our NDVI-profile map unit I-IV and the published biome maps ranges from 69,8 to 93,3. Unsurprisingly, the highest agreement is obtained in the map with the lowest number of biomes (2) and the lowest in the map with the highest number of units (4) (Table 2). In other words, there is a reasonable agreement ($\geq$70) between published biome maps and our biome map if 2–3 biomes are distinguished within Namibia.

3.3. Ecoregion level

Six published ecoregion maps have a similar number of units (Table 1). However, their legends contain inconsistent combinations of vegetation attributes including structure, plant species assemblages and/or landscape features. The ecoregions boundaries are of two types, namely the zigzag lines in vectorized raster maps (Fig. 5: green, partly; Fig. 6: black line and 8-Groups background) and smooth lines in vector maps (Fig. 5: black, blue and red). The map by Leser (1976) is adopted from Giess (1971) with a minor relocation of some boundaries and will not be part of further comparison. The map by Mendelsohn et al. (2002b) seems based on Giess, but shows additional, more detailed boundaries along some rivers, in the Cuvelai and the Succulent Karoo (Fig. 4: green boundaries). One unit runs from northwest to southeast coinciding largely with the Nama-Karoo biome (Fig. 3), while Giess divides this area north to south in three units and White (1983) shows a west to east gradient parallel to the coast. More inland, the boundaries by White become more north-south oriented, which corresponds largely with Giess. White divides the forest savanna and woodland area of Giess in the northwest (Fig. 5: black boundary) in two sub-units with an east-west oriented boundary. Another unit of Giess in the central-north is divided by White into 3 mapping units in a gradient parallel to the coast (Fig. 5: blue boundary). Both distinguish the wider Windhoek area as mountain or highland (wooded) savanna. The WWF ecoregion boundaries seem to be based on White (1983). The coastal Namib Desert is divided by WWF into 3 ecoregions with boundaries perpendicular to the coast (Fig. 5: red boundaries). The Karoo shrubland unit in the central-south of White's map (Fig. 5: blue boundaries) is also divided with a boundary perpendicular to the coast by WWF (Fig. 5: red boundaries) into two units, namely Nama-Karoo in the south and Namibian savanna woodlands in the north. Three of White's units (Fig. 5: blue boundaries) in the central-east are combined by WWF (red boundaries) into one. The boundaries of our NDVI-profile ecoregion map seem similar to Mendelsohn et al. (2002c) at certain places,

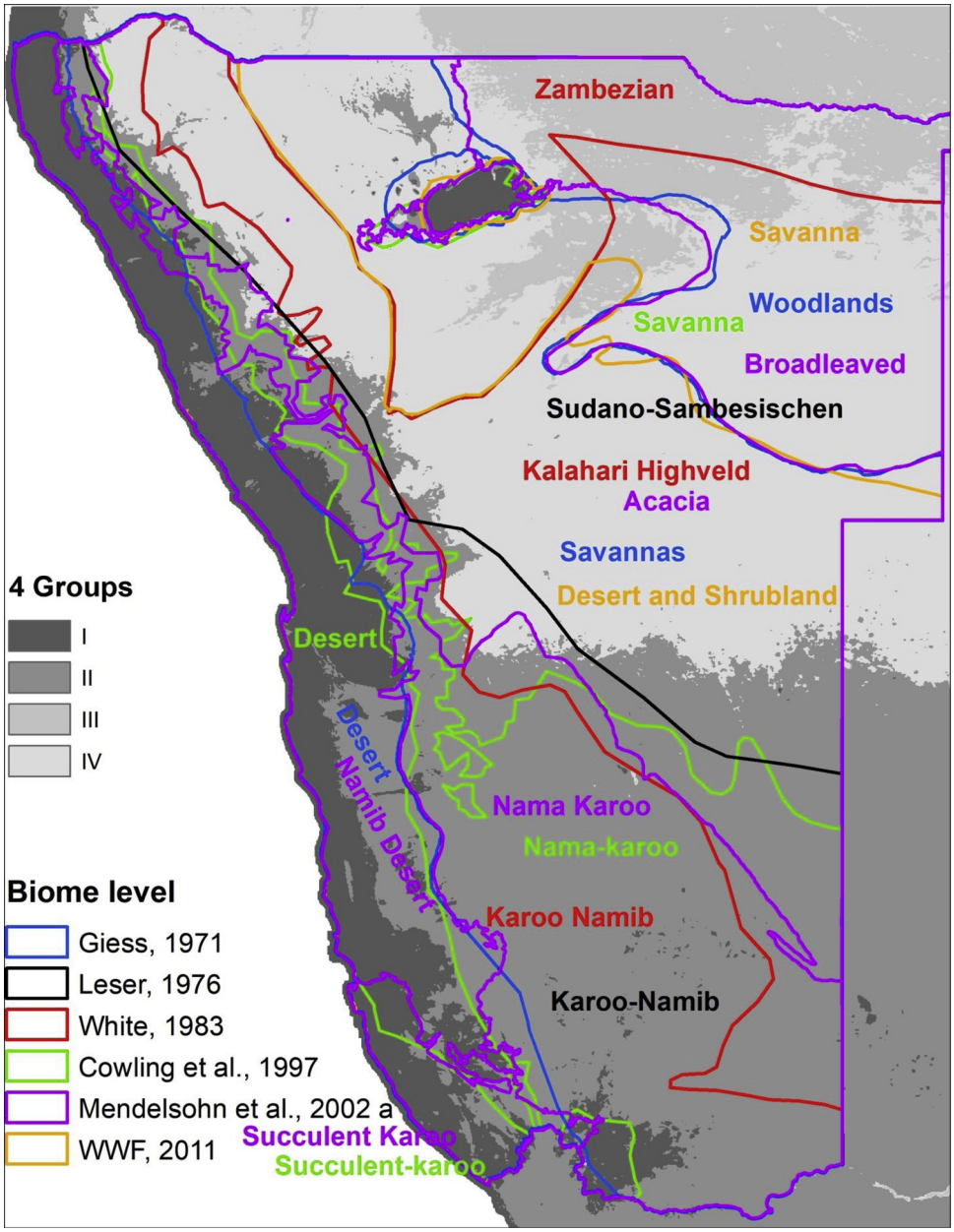

Fig. 4. The overlay of the six published biome level maps of Table 1 (colored lines and lettering) and the biome level NDVI-profile cluster-groups (background in grey tones).

Table 2
Agreement index calculated by a confusion matrix at the biome level between NDVI cluster-groups (Figs. 3 and 4) and published maps. Merged (heading second column) refers to the number of mapping units after mergers.

Published maps (Table 1)	Merged	Agreement
Giess (1971)	3	79,5
Leser (1976)	2	93,3
White (1983)	3	73,7
Cowling et al. (1997)	3	85,6
Mendelsohn et al. (2002)	4	69,8
WWF (2011)	2	77,5

especially in the arid south and west (Fig. 5). The ecoregion boundary lines of Mayaux et al. (2004) appear most similar in shape to those of the NDVI-profile map. However, river valleys and other subdivision perpendicular to the coast are mapped within the Namib Desert (Fig. 6: yellow background; black boundaries) by Mayaux et al. (2004).

The distinction between ecoregion E and F was not present on any of the published maps and therefore these have been combined in all map comparisons. The Etosha salt pan ecoregion was combined with its neighbouring ecoregion H for the comparison with the rainfall zone map. For the comparison with Giess'map (1971) the ecoregions G and H were combined; for Mayaux et al. (2004) the ecoregions C and G were combined. This resulted in either 6 or 7 merged units (Table 3). The positional agreement between our ecoregion map units A-H and the published ecoregion maps ranges from 51.0 to 74.6 (Table 3); the agreement with the rainfall zones (69,9) lies at the higher end of the range. The highest agreement is shown by the map by Mayaux et al. (2004). At ecoregion level, the agreement values are substantially lower than at biome level, if only because of the higher number of map units at ecoregion level.

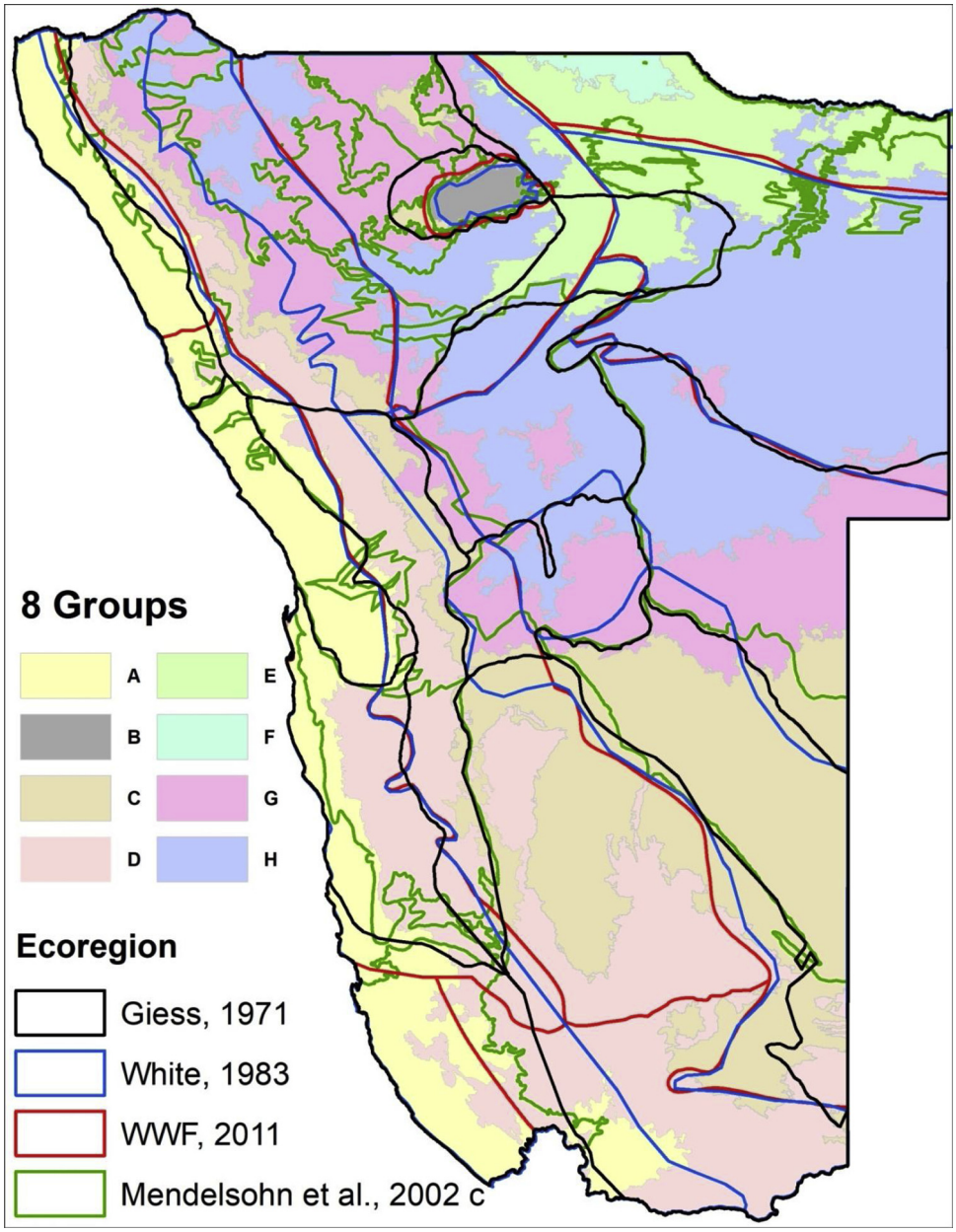

Fig. 5. The ecoregion level NDVI-profile cluster-groups (A-H) overlaid with the boundaries of the published equivalents in vector format (Giess, White, WWF and Mendelsohn).

3.4. The 81-cluster map

The maps depicting the optimal number of temporal NDVI-clusters and its vectorization are presented in Figs. 8 and 9 respectively. The associated temporal NDVI-profiles can be seen in Fig. 7. Seven small polygons of the vectorized 81-cluster raster map were merged with neighbouring larger polygons in and around Etosha. Subsequent clipping of the vector map with the Namibian boundary eliminated one unit at the coast line and 7 units along the border with Angola and South Africa. This elimination resulted in a vector map with 65 legend units in Namibia. None of the published countrywide Namibian vegetation maps contains a similar spatial detail, not even the map by Mayaux et al. (2004) which was prepared with temporal NDVI imagery of the same spatial resolution as our maps. The biome/ecoregion nomenclature does not yet include a generally accepted name for spatial units at a more detailed hierarchical level. In some cases, the term "vegetation complex" or "ecoregion subunits" has been used. As both seem confusing labels for different reasons (see Discussion), we refer to our optimal number of cluster products as 81-cluster map and 65-unit map. We purposely refrained from labelling our legend units in terms of vegetation attributes as even on the biome and ecoregion level the number of contrasting nomenclatures is bewildering (e.g. Fig. 3). Obviously, the 81-cluster map reflects the rainfall gradient (Fig. 8) from the coast to the northeast in more detail than the ecoregion level map (Fig. 4). However, this zonal pattern shows a range of azonal intermissions. Most distinct are the episodically flooded Etosha salt pan and the Cuvelai basin in the central-north, sandy regions within the Namib Desert and the Weissrand Plateau (white bare rock) in the central south (Fig. 8).

Evidently, the vegetation of the freehold ranches in the central and southern half of the country has similar temporal NDVI-profiles as contiguous unfarmed vegetation. Therefore neither farm, nor protected area boundaries are depicted at our map. Even the maize-triangle, the largest freehold block of rainfed and partly overhead-irrigated farms

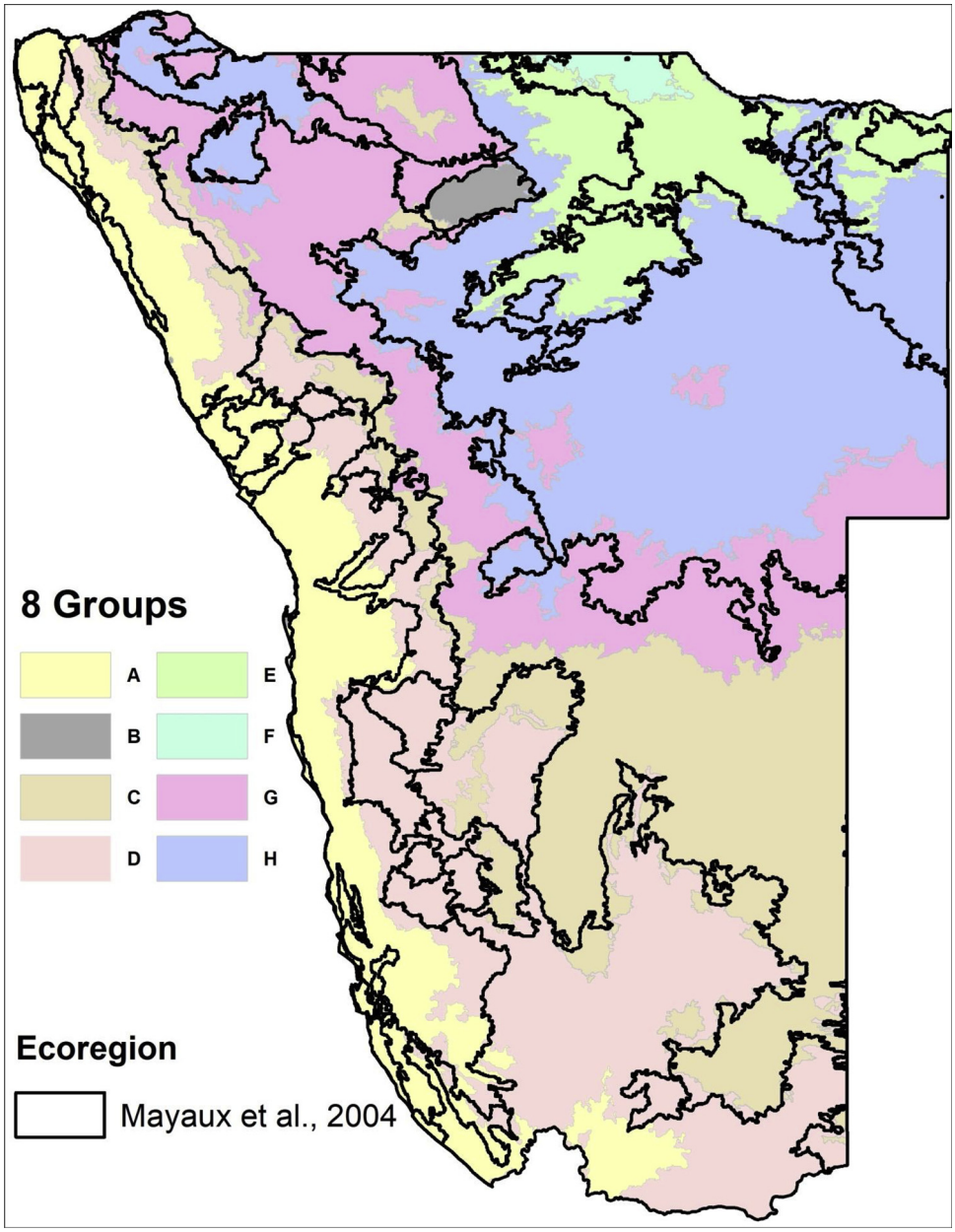

Fig. 6. The ecoregion level NDVI-profile cluster-groups (A-H) overlaid with the boundaries of the published map by Mayaux et al. (2004); both in raster format. Both vector maps show in the boundaries their raster map origin.

Table 3
Overall agreement calculated by a confusion matrix at the ecoregion level of the 8 NDVI cluster-groups (Fig. 3: A–H) with the published equivalents (Table 1) and with an annual rainfall map (last row). Merged (heading second column) refers to the number of mapping units after mergers.

Published maps (Table 1)	Merged	Agreement
Giess (1971)	6	66.0
White (1983)	7	62.1
WWF (2011)	7	53.0
Mayaux et al. (2004)	6	74.6
Mendelsohn et al. (2002)	7	59.6
Namibia Resource Consultants (1999)	6	69.8

(about 1500 km^2) cannot be distinguished on our 81-cluster map. Similarly, rainfed small-holdings seem to present the same temporal NDVI-profile as the adjacent uncultivated vegetation, except along the Cuvelei section of the Angolan border. The two largest cities, Windhoek and Rundu are visible (Fig. 8), but smaller than the minimum mapable unit.

The temporal NDVI-profile line graphs (Fig. 7) show the highest NDVI values for most units in the period from mid-February to the beginning of May, i.e. in the second half of the summer-rain season. The peak NDVI shifts gradually from February to April from the highest curve (top; turquoise) to the Karoo-Namib curves (rose). Collectively, the lowest NDVI values are reached toward the end of the dry, winter season in the second half of August and September. Several units differ from this general trend. The Etosha salt pan ecoregion (grey) has very low NDVI values without apparent amplitude, implying seasonally erratic greening of this edaphic desert. The Namib Desert ecoregion units (yellow) have very low NDVI amplitudes with a winter maximum (April-August), although at a low level. The semi-arid Karoo-Namib ecoregion units (rose) have the next lower NDVI amplitude. Here, the slightly higher NDVI values occur in the April-May period i.e. early winter indicating sporadic winter showers. From here on in the graph

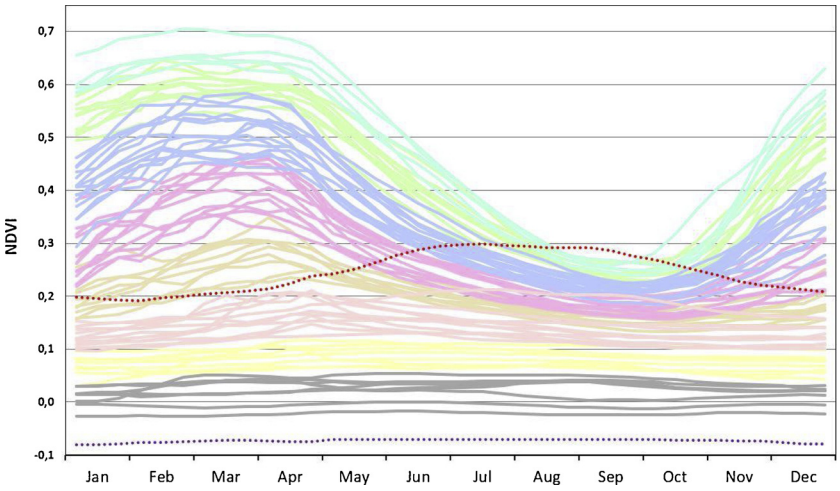

Fig. 7. The line graphs show the temporal NDVI-profiles of the 81-clusters (Fig. 8) in the colors of the 8 ecoregions (Figs. 5 and 6), thus illustrating the nested hierarchy of the ecoregion and the 81-cluster map. Clusters 55 (dotted red) and cluster 9 (dotted purple) were eliminated (Fig. 3). The grey lines at the bottom represent the sparse to non-existent green biomass of the Etosha salt pan. The yellow lines represent the coastal Namib Desert resulting from near zero annual rainfall. The bundle of turquoise and green lines at the top represents the sub-humid ecoregions with over 500 mm of summer-rain.

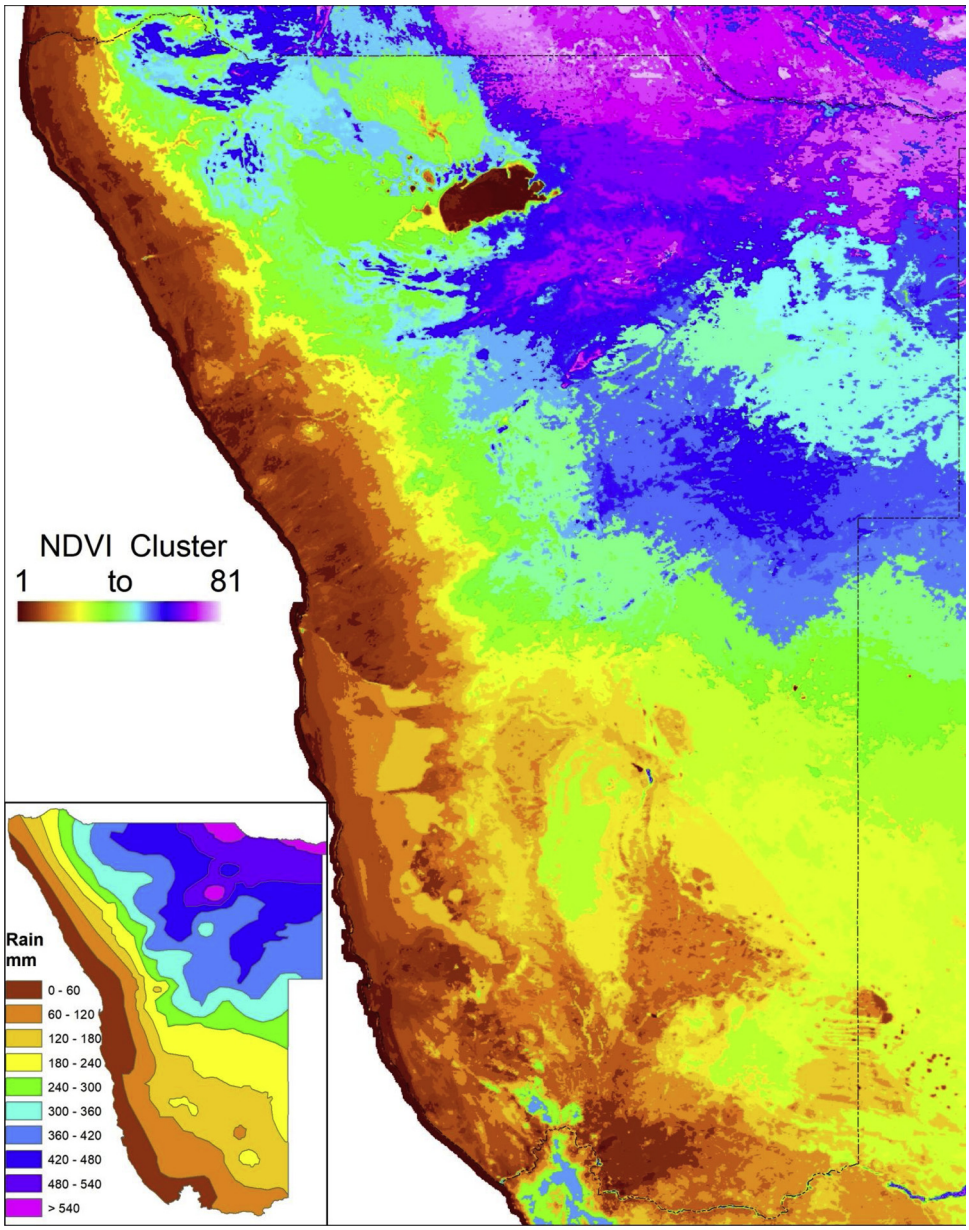

Fig. 8. The map shows the distribution of the optimal number of temporal NDVI clusters (81). For comparison, the average annual rainfall in mm is shown in the insert map.

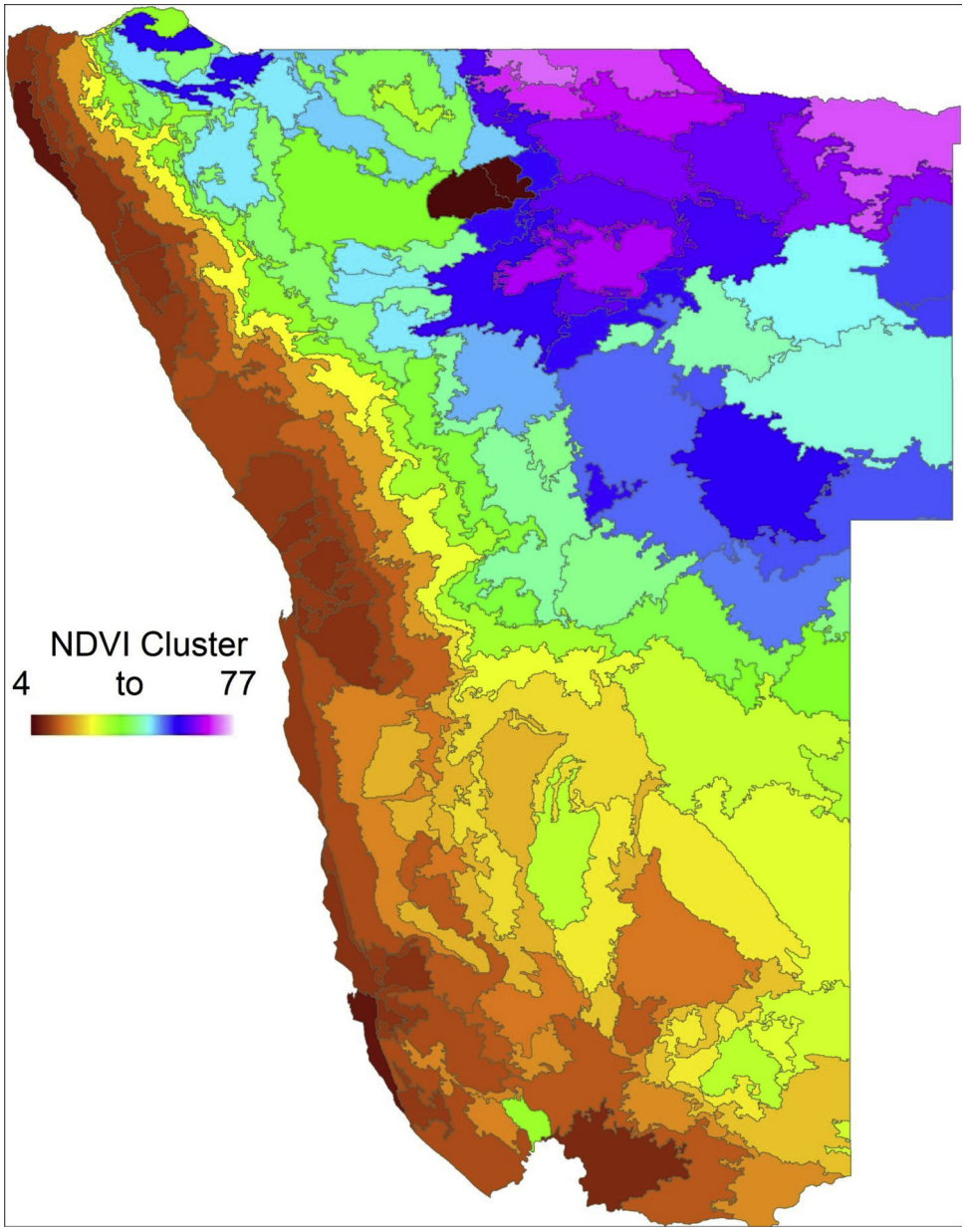

Fig. 9. Vector version of the 81-cluster raster map (Fig. 8) with 65 mapping units. The color scheme of Fig. 8 has been applied to facilitate the comparison of the maps and visualize the rainfall gradient (Fig. 8 insert map). The clusters 1,2,3,6,7,8,9,11,12, 55, 71,73,78–81 were eliminated.

(Fig. 7), the higher the NDVI values, the larger the amplitudes of the curves and the wider the distance of the adjacent lines in the graph. Most curves run in parallel for their full length. However, some lines cross once or twice an adjacent line once or twice for a period of one to two months, especially in the early summer period (November-December) indicating a differential start of greening. The two dotted lines (purple and red) substantially deviate from the set (Fig. 7) and represent a cluster in Etosha salt pan and a cluster on the coast at the southern border of Namibia. The salt pan cluster shows the lowest NDVI value in the graph, i.e. the absence of green vegetation. The other demonstrates higher green biomass during winter than in summer in contrast to most other profiles.

4. Discussion

Neither the techniques (ISODATA clustering, temporal profiling of NDVI and Hierarchical Clustering Analysis) nor coarse resolution hyper-temporal NDVI imagery are new. However, the consecutive use of these techniques on hyper-temporal NDVI imagery in countrywide vegetation mapping is a novelty.

Three nested, hierarchical levels of vegetation mapping units were extracted from hyper-temporal NDVI imagery. All published Namibian vegetation maps present a single or dual hierarchical level that is either biome, ecoregion or both. Our approach extracts a third, more detailed level with 81 mapping units from hyper-temporal coarse resolution satellite imagery. Similar imagery (NOAA-AHVRR) has been available since about 1980 and was used by Higgins et al. (2016) for global biome mapping. The number of mapping units at biome level of our NDVI-profile based map (4) falls within the range of those in the published maps (2–5). In contrast, the number of ecoregions based on NDVI-profiles (8) is smaller than in the published cases (10–14). The higher number of ecoregions in the published maps is located in the coastal Namib Desert and the semi-arid Karoo-Namib in the south. In these relative arid conditions, the NDVI-profile shows little variation between areas and seasons (Fig. 7: grey lines). However, none of the published ecoregion maps captured the spatial diversity in vegetation cover

detected by our approach in the northeastern Mega-Kalahari. In other words, most published ecoregion level maps use the level of spatial information provided by coarse resolution NDVI imagery inconsistently across the country. Similar spatial inconsistencies, although at finer scales have been reported from Namibia by Ullerud et al. (2018).

The agreement indexes calculated for biomes demonstrate that these were distinguished reasonably well without resort to hyper-temporal satellite imagery and modern cluster methods for raster data. However the number of biomes and the delineation of their boundaries appeared arbitrary. The lower agreement indexes for ecoregions suggest that these may be much better delineated by clustering of satellite imagery. The highest ecoregion map agreement (74.6) was calculated for the map of Mayaux et al. (2004). However, the agreement index depends on the number of legend units, in this case 6 versus 7 for other maps (Table 3). We may expect a 5–10 % loss of agreement index value with each additional legend unit (Westinga, 2004). Thus, the Mayaux et al. (2004) and Giess (1971) maps matched best with our ecoregion level product. The first is partly based on temporal NDVI-profiles, although differently constructed than ours and seemingly without first-hand field knowledge of Namibia. The first map is based on a decade of field survey (Giess, 1971).

Our temporal NDVI-profile based map and the Mayaux et al. (2004) map are in raster format and represent continuous fields in contrast to the published maps in vector format that present discrete, categorical information. Consequently, vector maps include virtual lines representing fuzzy boundaries which cannot be recognized on the ground or imagery. One of the Mendelsohn et al. maps (2002c) shows regional patterns similar to our ecoregion level map and in other parts to the Mayaux et al. maps (2004) suggesting Mendelsohn et al. used NDVI satellite image as well for their vector map.

The nomenclatures of the published biome maps refer explicitly to geographical features (zone, region, choria or biome). The more arid biomes carry established southern-African toponyms older than the published maps (Namib [Desert]; Karoo; Kalahari Highveld). Those in the more humid areas refer in their legend labels to vegetation structure (savanna, woodland, shrubland, Acacia) or Africa-wide biogeographical zones ([Sudano-] Zambezi; Fig. 4). The “ecoregion” label first appears for the intermediate level of the nested, spatial hierarchy in 2011 in our map set. Earlier, “vegetation type” was the label of choice (Table 1). A disadvantage of the latter term seems that from a classical vegetation science perspective, a mapping unit is more often than not a complex of vegetation types, be it floristically or structurally defined. The term ecoregion better captures the geographic nature and complexity of mapping units.

Our 81-mapping unit raster map (Fig. 8) and its 65-mapping unit vector version (Fig. 9) show a SW-NE gradient that corresponds with the rainfall gradient of 0–600 mm per year (Cowling et al., 1997; du Plessis, 1999). Relatively small interruptions of this gradient may be detected, but many of them are smaller than the minimum mapable unit at the selected map scale. The main azonal interruption is Etosha salt pan (about 5000 km^2) visible at all three hierarchical levels and mapped by various authors as separate biome or ecoregion (Table 1). Rainfall clearly overrules variation in temperature in its impact on temporal NDVI-profiles which may be explained by the linear correlation of rainfall and vegetation production at annual rainfall below 600 mm per year (Walter, 1973; Penning de Vries and Djiteye, 1982; du Plessis, 1999) as applies to Namibia. Given this rainfall range, the increase in NDVI in our 65 and 81 unit maps from the SW to the NE might be partially attributed to an increase in green biomass during the summer rain season. The correlation of snapshot and hyper-temporal NDVI values have been locally established in Namibia. Green biomass estimations of trees, shrub and grass on the ground have shown a high correlation with NDVI values of snapshot 1 km resolution NOAA-AVHRR images in Etosha National Park (Sannier et al., 2002). Further, analysis of six year hyper-temporal SPOT VGT MVC of 1 km resolution has shown a good correlation with the coverage of woody vegetation canopy estimated on Landsat-7 ETM calibrated with ground samples across a transect covering 6 ecoregions (Wagenseil and Samimi, 2007).

Seasonal NDVI-profiles at 1 km resolution have been linked to single structural vegetation types (Mayaux et al., 2004). However, more than one structural vegetation types frequently occurs within a 1 km raster (Foody et al., 1997). This also applies to Namibia. For example, the Cuvelai consists of a mosaic of small water bodies, salt pans, grassland, crop fields and barrens, at the 1 km resolution. Another illustrative case is the longitudinal dune field in the eastern Kalahari covered with grass and trees on the dunes and shrub in the interdunal valleys; both dunes and valleys are 50 − 500 m wide. To distinguish and map individual, homogenous structural vegetation types in the above examples, will require finer resolution imagery and equivalent map scales. For example, the 20 m resolution map of ESA (2017) for Namibia separates smaller spatial units within complex mapping units at coarser resolution. However, this results at ecoregion and biome scale in a multitude of salt and pepper patches consisting of 2, 3 or 4 vegetation cover classes. Such detail leaves map generalization to the user.

The NDVI values between neighbouring temporal profiles differ most during the second half of the summer-rain period (Fig. 7). Therefore, this period would seem the best choice for detection of vegetation units on snapshot imagery. However, cloud-free imagery would be scarcer during summer rains. The peak NDVI values that shift from February to April may indicate a gradient in the start of the vegetation growing season from early in the NE to later in the SW as well as a gradient in rainfall (Fig. 8: insert). The temporal NDVI profile of the Namib-Desert and the semi-arid Karoo-Namib suggest a slight mediterranean winter-rain regime as an outlier of the South African Western Cape climate. The ultimate mediterranean rainfall pattern is expressed in the one of the temporal NDVI-profiles (Fig. 7: dotted red line). A mediterranean rainfall pattern is likely to be associated with assemblages of succulent-leaved low plants as reflected in the label of the Succulent-Karoo biome (Fig. 4). The crossing NDVI curves demonstrate that a certain number of vegetation units identified by temporal NDVI-profiles may not be detected at snapshot imagery depending on the date of the imagery.

5. Conclusion and recommendations

Our 4 cluster-groups (I-IV) correspond broadly with the available vector biome maps in their number of units (2–5). However, the position of the biome boundaries varies considerably between the maps, particularly between a savanna and woodland biome. Our 8 cluster-groups (A-H) show a somewhat smaller number of map units than the published equivalents (10–14). This is the result of the similarities between the temporal NDVI profiles in the (semi-)arid regions. Similarly to the biome, the ecoregion boundaries vary considerably across the published maps. At both levels, mapping unit boundaries seem to have been arbitrarily drawn in the published maps, while the vegetation attributes have not been sampled and recorded systematically. Finally, our ecoregion unit level map relate well to rainfall zones. Our 81-cluster map has no equivalent in the published maps and has potential as a base for a more detailed countrywide vegetation mapping.

Our proposed mapping method is reproducible for the resulting number of units and boundaries at three hierarchical levels. The units (temporal NDVI-profiles) may be translated into meaningful vegetation mapping units by analysis of observational vegetation data. Spatially comprehensive, countrywide census data of tree species presence (Curtis and Mannheimer, 2005) and grasses (Klaassen and Craven, 2003) are available and may be analyzed for this purpose (van Gils, 2015).

Author statement

On behalf of the co-authors, Ana Patricia Ruiz Beltran, Cees de Bie and Hein van Gils, I confirm that this manuscript, neither in part nor in

whole, has been published elsewhere nor is it under consideration for publication by any other journal. Additionally, we have no conflict of interest to disclose. Hence, we kindly request you to consider the manuscript for publication.

Declaration of Competing Interest

On behalf of the co-authors, Ana Patricia Ruiz Beltran, Cees de Bie and Hein van Gils, I confirm that this manuscript, neither in part nor in whole, has been published elsewhere nor is it under consideration for publication by any other journal. Additionally, we have no conflict of interest to disclose. Hence, we kindly request you to consider the manuscript for publication.

Acknowledgments

The Mexican National Council of Science and Technology (CONACYT), through the South Lower Californian Council of Science and Technology (COSCYT) funded the contribution of Ana Patricia Ruiz-Beltran.

References

Ali, A., de Bie, C.A.J.M., Skidmore, A.K., Scarrott, R.G., Hamad, A.A., Venus, V., Lymberakis, P., 2013. Mapping land cover gradients through analysis of hyper-temporal NDVI imagery. Int. J. Appl. Earth Obs. Geoinf. 23, 301–312. https://doi.org/10.1016/j.jag.2012.10.001.

Cowling, R.M., Richardson, D., Pierce, S.M. (Eds.), 1997. Vegetation of Southern Africa. Cambridge University Press, Cambridge, UK.

Curtis, B., Mannheimer, C., 2005. Tree Atlas of Namibia. National Botanical Research Institute, Windhoek, Namibia.

de Bie, C.A.J.M., Khan, M.R., Smakhtin, V.U., Venus, V., Weir, M.J.C., Smaling, E.M.A., 2011. Analysis of multi – temporal SPOT NDVI images for small – scale land – use mapping. Int. J. Remote Sens. 32 (21), 6673–6693. https://doi.org/10.1080/01431161.2010.512939. 2011.

de Bie, C.A.J.M., Nguyen, T.T.H., Ali, A., Scarrott, R., Skidmore, A.K., 2012. LaHMa: a landscape heterogeneity mapping method using hyper-temporal datasets. Int. J. Geogr. Inf. Sci. 26, 2177–2192. https://doi.org/10.1080/13658816.2012.712126.

du Plessis, W.P., 1999. Linear regression relationships between NDVI, vegetation and rainfall in Etosha National Park, Namibia. J. Arid Environ. 42, 235–260. https://doi.org/10.1006/jare.1999.0505.

ESA, 2017. Improving Land Cover Mapping With Sentinel-2. Retrieved from. http://www.esa.int/Our_Activities/Observing_the_Earth/Improving_land_cover_mapping_with_Sentinel-2.

FAO, 2017. Hyper-temporal Remote Sensing to Support Agricultural Monitoring. Retrieved from. http://www.fao.org/elearning/#/elc/en/courses/GDLM.

Foody, G.M., Lucas, R.M., Curran, P.J., Honzak, M., 1997. Mapping tropical forest fractional cover from coarse spatial resolution remote sensing imagery. Plant Ecol. 131, 143–154. https://doi.org/10.1023/A:1009775619936.

Giess, W., 1971. A preliminary vegetation map of South West Africa. Dintera 4, 1–114. map retrieved from. http://www.the-eis.com/.

Girma, A., de Bie, C.A.J.M., Skidmore, A.K., Venus, V., Bongers, F., 2016. Hyper-temporal SPOT-NDVI dataset parameterization captures species distributions. Int. J. Geogr. Inf. Sci. 30, 89–107. https://doi.org/10.1080/13658816.2015.1082565.

Higgins, S.I., Buitenwerf, R., Moncrieff, G.R., 2016. Defining functional biomes and monitoring their change globally. Glob. Change Biol. 22, 3583–3593. https://doi.org/10.1111/gcb.13186.

Hüttich, C., Gessner, U., Herold, M., Strohbach, B.J., Schmidt, M., Keil, M., Dech, S., 2009. On the suitability of MODIS time series metrics to map vegetation types in dry savanna ecosystems: a case study in the Kalahari of NE Namibia. Remote Sens. 620–643. https://doi.org/10.3390/rs1040620.

Khan, M.R., de Bie, C.A.J.M., van Keulen, H., Smaling, E.M.A., Real, R., 2010. Disaggregating and mapping crop statistics using hypertemporal remote sensing. Int. J. Appl. Earth Obs. Geoinf. 12, 36–46. https://doi.org/10.1016/j.jag.2009.09.010.

Klaassen, E.S., Craven, P., 2003. Checklist of Grasses in Namibia. Southern African Botanical Diversity Network Report No. 20. SABONET, Pretoria and Windhoek.

Leser, H., 1976. Südwestafrika: eine geographische Landeskund. SWA Wissenschaftliche Gesellschaft, Windhoek.

Lillesand, T.M., Kiefer, R.W., Chipman, J.W., 2004. Remote Sensing and Image Interpretation, 7th ed. Wiley & Sons, New York.

Mayaux, P., Bartholomé, E., Fritz, S., Belward, A., 2004. A new land-cover map of Africa for the year 2000. J. Biogeogr. 31, 861–877. https://doi.org/10.1111/j.1365-2699.2004.01073.x.

Mendelsohn, J., Jarvis, A., Roberts, C., Robertson, T., 2002. Atlas of Namibia: a Portrait of the Land and Its People. shapefiles: biome (a), vegetation type (b) and vegetation structure (c). Retrieved from. David Philip, Cape Town, South Africa. http://www.the-eis.com/.

Mugabowindekwe, M., Muyizere, A., Li, F., Yunfeng, Q., Rwanyiziri, G., 2018. Application of multi-temporal MODIS NDVI data to assess practiced maize calendars in Rwanda. J. Resour. Ecol. 9, 273–280. https://doi.org/10.5814/j.issn.1674-764x.2018.03.007.

Namibia Resource Consultants, 1999. Rainfall Distribution in Namibia: Data Analysis and Mapping of Spatial, Temporal, and Southern Oscillation Index Aspects. Ministry of Agriculture, Water and Rural Development, Windhoek.

Nguyen, T.T.H., De Bie, C.A.J.M., Ali, A., Smaling, E.M.A., Chu, T.H., 2011. Mapping the irrigated rice cropping patterns of the Mekong delta, Vietnam, through hyper-temporal SPOT NDVI image analysis. Int. J. Remote Sens. 33, 415–434. https://doi.org/10.1080/01431161.2010.532826.

Penning de Vries, F.W., Djiteye, M.A., 1982. La productivité des pâturages sahéliens: une étude des sols, des végétations et de l'exploitation de cette ressource naturelle. Pudoc, Wageningen, The Netherlands.

Sannier, C.A.D., Taylor, J.C., Du Plessis, W., 2002. Real-time monitoring of vegetation biomass with NOAA-AVHRR in Etosha National Park, Namibia, for fire risk assessment. Int. J. Remote Sens. 23, 71–89. https://doi.org/10.1080/01431160010006863.

Swain, P.H., 1973. Pattern Recognition: a Basis for Remote Sensing Data Analysis. Laboratory for Applications of Remote Sensing (LARS), Purdue University, West Lafayette, Indiana.

Tou, J.T., Gonzalez, R.C., 1974. Pattern recognition principles. Reading. Addison Wesley, Massachusetts.

Ullerud, H.A., Bryn, A., Halvorsen, R., Hemsing, L.O., 2018. Consistency in land- cover mapping: influence of field workers, spatial scale and classification system. Appl. Veg. Sci. 21, 278–288 10.111/avsc.12368.

van Gils, H.A.M.J., 2015. Web-based biodiversity geodatabases for environmental assessment in mid-income Namibia. In: International Association for Impact Assessment; IAIA15 Impact Assessment in the Digital Era. Conference Proceedings, Florence. . http://conferences.iaia.org/2015/final_papers.php.

van Gils, H.A.M., van, J., Batsukh, O., Rossiter, D.G., Munthali, W., Liberatoscioli, E., 2008. Forecasting the pattern and pace of *Fagus* forest expansion in Majella national park, Italy. Appl. Veg. Sci. 11, 539–546.

van Gils, H.A.M.J., Westinga, E., Carafa, M., Antonucci, A., Ciaschetti, G., 2014. Where the bears roam in Majella National Park, Italy. J. Nat. Conserv. 22, 23–34.

van Gils, H.A.M.J., Bennett, R.M., Hipondoka, M., 2015. Of pastures and tourism; A comparison of Tyrolean and Namibian commons institutions. In: Grüne, N., Hübner, J., Siegel, G. (Eds.), Rural Commons: Collective Use of Resources in the European Agrarian Economy. Studienverlag G.m.b.H., Innsbruck, pp. 258–273 (Jahrbuch für Geschichte des ländlichen Raumes; No. 12).

Wagenseil, H., Samimi, C., 2007. Woody vegetation cover in Namibian savannahs: a modelling approach based on remote sensing. Erdkunde 61, 325–334. https://doi.org/10.1080/01431161.2014.883104.

Walter, H., 1973. Vegetation of the Earth in Relation to Climate and the Eco-physiological Conditions. English Universities Press.

Walter, H., 1976. Die ökologische Systeme der Kontinente (Biogeosphäre). Gustav Fischer Verlag, Stuttgart.

Wessels, K., Steenkamp, K., von Maltitz, G., Archibald, S., 2011. Remotely sensed vegetation phenology for describing and predicting the biomes of South Africa. Appl. Veg. Sci. 14, 49–66. https://doi.org/10.1111/avsc.2011.14.issue-1.

Westinga, E., 1989. Application of geographical information systems and remote sensing for monitoring landuse changes in the Phu Wiang watershed, Thailand. In: Proceedings of Franco-Thai Workshop on Remote Sensing, Nov 2–4, 1989. KhonKaen, Thailand.

Westinga, E., 2004. 50 years monitoring land cover and use of the Phu Wiang watershed, Thailand. In: ACRS 2004: Proceedings of the 25th Asian Conference on Remote Sensing, ACRS 2004 Silver Jubilee: November 22–26, 2004. Chiang Mai, Thailand. Chiang Mai: Geo-Informatics and Space Technology Development Agency (GISTDA). pp. 940–945.

White, F., 1983. The Vegetation of Africa, a Descriptive Memoir to Accompany the UNESCO/AETFAT/UNSO Vegetation Map of Africa. map retrieved from. UNESCO, Paris. http://esdac.jrc.ec.europa.eu/images/Eudasm/Africa/images/maps/download/veg2.jpg.

WWF, 2011. Terrestrial Ecoregions. Retrieved from. https://worldmap.harvard.edu/data/geonode:wwf_terr_ecos_oRn.